

First-principles determination of exchange interactions in delafossite $YCuO_{2.5}$

O. Le Bacq* and A. Pasturel

Laboratoire de Physique et Modélisation des Milieux Condensés, CNRS, Boîte Postale 166, 38042 Grenoble, France

C. Lacroix

Laboratoire Louis Néel, CNRS, Boîte Postale 166, 38042 Grenoble Cedex 9, France

M. D. Núñez-Regueiro

Laboratoire de Physique des Solides, CNRS-UMR 8502, Bâtiment 510, Université Paris-Sud, 91405 Orsay, France

(Received 29 September 2004; published 25 January 2005)

We perform a first-principles calculation within the local density approximation (LDA)+U approximation for the delafossite $YCuO_{2.5}$, which up to now was considered as a sawtooth lattice. The magnetic interactions are mapped onto a Heisenberg model whose exchange interactions are fitted to first principles total energy calculations for different spin configurations. Four interactions appear to have a significant value. While interplane interactions can be safely neglected, interchain interactions are much smaller than intrachain ones, confirming the low-dimensional character of this system. Besides the nearest-neighbor intrachain antiferromagnetic interactions, we find two unexpected ferromagnetic interactions that can play an important role. The results are discussed in relation with recent experimental data.

DOI: 10.1103/PhysRevB.71.014432

PACS number(s): 75.10.Hk, 71.15.Nc

I. INTRODUCTION

Since the proposal by Anderson of a resonating valence bond (RVB) state in triangular lattices of spins $1/2$, the search for real systems with these characteristics has not stopped. Recently, several examples with peculiar physics related to quantum spins in a triangular geometry have been discussed: huge thermopower in Na_xCoO_2 , unexpected superconductivity in hydrated samples, and the puzzling absence of ordering in $LiNiO_2$ in contrast with isomorphous $NaNiO_2$. Another interesting family is the $RCuO_{2+\delta}$ ($R=Y, La$, etc.) delafossites, which depending on the oxygen over-doping δ , give rise to different triangular-based lattices with frustrated interactions between the induced Cu^{2+} ions.¹ Preliminary studies of the effective diluted kagomé lattices for $x=2.66$ predicted interesting properties.²

Now, the synthesis of orthorhombic 2H single-phase samples of $YCuO_{2.5}$ has allowed one to elucidate its detailed crystallographic structure.³ The additional $x=0.5$ oxygen ions locate at the center of alternating sets of triangles (see Fig. 1), providing exchange O-Cu-O paths between $S=1/2$ spins on alternating Δ chains, therefore assumed to be nearly independent. Due to the smaller Cu-O-Cu angle these nearest-neighbor (NN) antiferromagnetic (AF) interactions are expected to be weaker than in the high temperature superconducting cuprates, but the prediction of further interactions is not evident. On the other hand, up to now, no magnetic ordering has been observed down to low temperature.

From Fig. 1 we can extract the simplified picture of the Cu-O plane shown in Fig. 2, which, considering only exchange paths through oxygen atoms, appears as a nice realization of the sawtooth lattice. In fact, the Cu chains have the topology of the sawtooth lattice in the sense that each Cu triangle is connected to the following triangle in the same chain by only one corner. When all bonds have the same AF interaction values this lattice is known to show remarkable

properties: a double degenerate dimer ground state, with kinks and antikinks pair-excitations and a k -independent reduced gap for the low-lying excitation modes.^{4,5} However, the measured angles and distances for $YCuO_{2.5}$ and the dif-

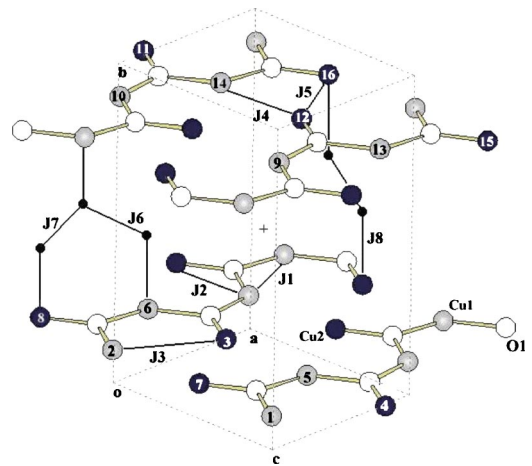


FIG. 1. Crystallographic structure of $YCuO_{2.5}$ and definition of the exchange-coupling parameters inside chains (J_1 , J_2 , and J_3), between chains (J_4 and J_5), and between planes (J_6 , J_7 , and J_8). Only Cu1 atoms (gray), Cu2 atoms (dark), and interstitial O1 atoms (white) in Cu planes are shown. While Cu1 (black circles) adopts tetrahedral coordination with two O ions in this plane (and with two other O ions out of the plane), Cu2 (gray circles) adopts triangular coordination with just one O in this plane. Selected O2 and O3 atoms which enter the path of super-super exchange-coupling in-between planes (J_6 , J_7 , and J_8) are spotted with small black dots. Y atoms (not represented) are enclosed in octahedra defined by O2 and O3 atoms. The primitive cell is shown with dotted lines. The labels of Cu atoms (enclosed in our simulation cell) are given at the center: atoms 1–8 belong to a first plane (A) and atoms 9–16 to a second plane (B).

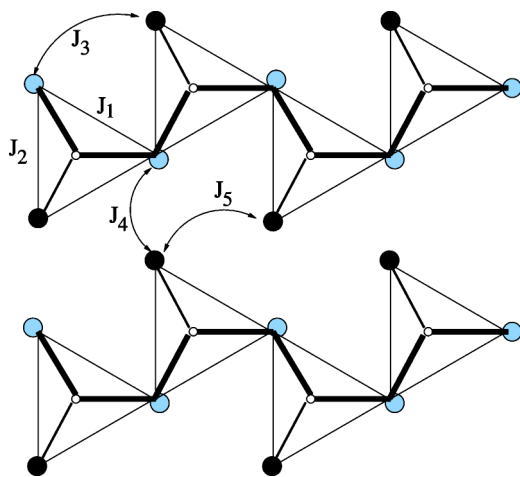


FIG. 2. Alternating chains in the triangular Cu planes of the delafossite $\text{YCuO}_{2.5}$. The extra O ions (white circles) for $x=0.5$ are located at the center of particular triangles of Cu ions, creating AF super exchange only within these triangles. This gives nearly independent Δ chains, indicated by thick black lines. Gray circles correspond to the basis of each triangle (these sites are shared with the following and previous triangles in the same chain and called Cu1 in the text), while black circles represent their vertex and are called Cu2 in the text.

ferent coordination of the Cu ions³ indicate different interactions between the two spins on the base J_1 and between the base-vertex NN spins J_2 of the triangles. In the absence of *ab initio* calculations for the AF interactions in $\text{YCuO}_{2.5}$, some of us have first studied the sawtooth lattice for various ratios J_1/J_2 .⁶ By exact diagonalization we have shown that the elementary excitation spectrum has a gap only $0.487 \leq J_1/J_2 \leq 1.53$. The gap, dispersionless for $J_1=J_2$, acquires increasing k -dependence as the ratio J_1/J_2 moves away from unity. We have also shown that the gap closure is related to the instability of the dimers in the ground state. For lower or higher interaction ratios the results approach those of the Heisenberg chain, with no gap and pairs of spinon excitations exhibiting a strongly dispersive spectrum.⁶

Although we can find in the literature many other nearly one-dimensional spin systems, $\text{YCuO}_{2.5}$ is especially interesting, since to our knowledge, it could correspond to the first experimental example of a Δ chain with Sutherland-Shastry type excitations.⁷ We perform here a first-principles study for the delafossite $\text{YCuO}_{2.5}$ in order to determine the exchange interactions and to check the generally assumed one-dimensional character of this system. Section II contains the description of our theoretical approach. Section III provides the results concerning the electronic structure. We show that, contrary to the local density approximation (LDA), the LDA+U is able to reproduce the experimentally observed magnetic structures, band gap, and experimental crystallographic parameters of the compound. Concerning the magnetic ground state, our calculations reveal the relevance of unexpected intrachain ferromagnetic interactions. Section IV gives a summary and the conclusions of this work.

II. THEORETICAL METHODS

A. The Hamiltonian

In the following we will show that this complicated system can be well-described by separating the electronic (H_0) and magnetic contributions in the Hamiltonian:

$$H = H_0 + \frac{1}{2} \sum_{\langle i,j \rangle} J_{ij} \mathbf{S}_i \cdot \mathbf{S}_j, \quad (1)$$

where the summation is over all distinct pairs, \mathbf{S}_i is the spin-vector on site i , and J_{ij} is the exchange-coupling between the moments on site i and j , to be determined. H_0 contains all the nonmagnetic effects.

We want to determine the relevant exchange interactions and calculate their values from first principles calculations. The idea behind our method is the following: suppose that the total energy of the system, E_r , can be separated into a nonmagnetic contribution (purely electronic) E_{nm} and a magnetic contribution that can be expressed through exchange interactions $E_m = \sum J_{ij} \mathbf{S}_i \cdot \mathbf{S}_j$, introducing as many exchange parameters as necessary. Then by calculating this total energy for several magnetic arrangements, it is possible to extract the values of the exchange interactions J_{ij} . This procedure assumes that the calculated magnitude of the magnetic moments do not depend on the magnetic structure, so it is expected to work well for localized spin systems, which is the case of $\text{YCuO}_{2.5}$. Although in Eq. (1) the J_{ij} interactions are Heisenberg-like, we restrict here to collinear magnetic configurations which are sufficient to determine their values. Of course, in a second step, the same parameters can be used to determine the precise nature of the ground state, i.e., if it is collinear or not. By looking carefully at the crystallographic structure, it appears that eight exchange interactions must be taken into account (see Fig. 1): three intrachain (J_1, J_2, J_3), two interchain (J_4, J_5), and three interplane interactions (J_6, J_7, J_8). Thus to be able to estimate these exchange interactions, it is necessary to study at least nine magnetic configurations. In fact we have studied 15 different collinear ordered magnetic ground states in order to check the validity of the method. If the energy of these 15 configurations can be fitted reasonably well by the same eight exchange interactions, the method can be considered as valid for this system. Similar approaches have been successfully applied before on very different systems.⁸⁻¹⁴

We can write the energy of our system as

$$E = E_0 + J_1/2 \sum_{i_1, j_1}^{16} (\mu_{i_1} \cdot \mu_{j_1})_{1\text{NN}} + J_2/2 \sum_{i_1, j_2}^{32} (\mu_{i_1} \cdot \mu_{j_2})_{2\text{NN}} + J_3/2 \sum_{i_1, j_2}^{16} (\mu_{i_1} \cdot \mu_{j_2})_{3\text{NN}} + \dots, \quad (2)$$

where i_1 and j_2 indexes run over Cu1 atoms and Cu2 atoms, respectively, so that μ_{i_1} is the moment of Cu1 atom located at site i and μ_{j_2} is the moment of Cu2 atom at site j . In Eq. (2), the multiplicities of the different types of spin pairs in the summation are the ones of the double primitive cell we used for the calculations, namely a 72 atoms cell including

16 Cu atoms displayed in Fig. 1. Inside chains, the exchange couplings between Cu nearest neighbors [J_1 and label 1NN in Eq. (2)] only involve Cu1 atoms (see Fig. 1). Two types of exchange-coupling interactions between Cu1 and Cu2 atoms may be distinguished inside chains. They are denoted J_2 and J_3 and correspond to the second (label 2NN) and third (label 3NN) nearest-neighbor distances with respect to Cu1 atoms. As Cu2 atoms inside the same chain present neither direct nor super or super-super exchange coupling between each other, their interaction is neglected in the present model.

In addition to these intrachain interactions, we include exchange coupling between chains and super-super exchange coupling between planes in order to investigate their influence on the magnetic ground state of this compound (see Fig. 1). For this purpose, we add the interactions between Cu1_{c1} and Cu2_{c2} atoms (J_4) and between Cu2_{c1} and Cu2_{c2} atoms (J_5), where c1 and c2 label two neighboring chains. Moreover, interplane interactions are taken into account by introducing the J_6 , J_7 , and J_8 exchange-coupling parameters, the Cu atoms involved in the exchange paths are shown in Fig. 1.

B. The first-principles method

All first-principles calculations were performed using the projector augmented wave (PAW) method^{15,16} as implemented in the Vienna *Ab-initio* Simulation Package (VASP) program.¹⁷ This is an all-electron method, based on the density functional theory (DFT),^{18,19} which allows a correct description of the valence wave functions and its nodal behavior without any shape approximation on the crystal potential. The PAW basis includes plane waves with a 414.3 eV cutoff and spherical-harmonic terms through $\ell_{max}=4$ inside the augmentation spheres. Calculations include the $Y(4s^2 4p^6 5s^2 4d^1)$, $Cu(3d^1 0 4s^1)$, and $O(2s^2 2p^4)$ atomic levels as valence states, while the remaining inner-shell electrons are treated within a rigid-core approximation.

The Vosko, Wilk, and Nusair interpolation²⁰ for the exchange-correlation potential is used within the local density approximation (LDA). The effects due to the localization of the d electrons of the Cu ions in the oxide are taken into account within the LDA+U approximation as recently implemented in VASP.^{21,22} In the so-called LDA+U approximation,²³ the spin-polarized LDA potential is supplied by a Hubbard-like term to account for the quasiatomic character of the localized (here Cu 3d) orbitals. Hence the localized electrons (Cu 3d) experience a spin- and orbital-dependent potential, while the other orbitals are delocalized and considered to be properly described by the LDA. Although the LDA+U is still a mean-field approach, it has the advantage of describing both the chemical bonding and the electron-electron interaction. The corrected functional has the following expression:²⁴

$$E_{LDA+U} = E_{LDA} + \frac{U-J}{2} \sum_{\sigma} \text{Tr}[\rho^{\sigma} - \rho^{\sigma} \rho^{\sigma}], \quad (3)$$

where ρ^{σ} is the on-site occupancy matrix, J is the screened exchange energy (approximation of the Stoner exchange parameter and almost constant for the 3d transition-metal

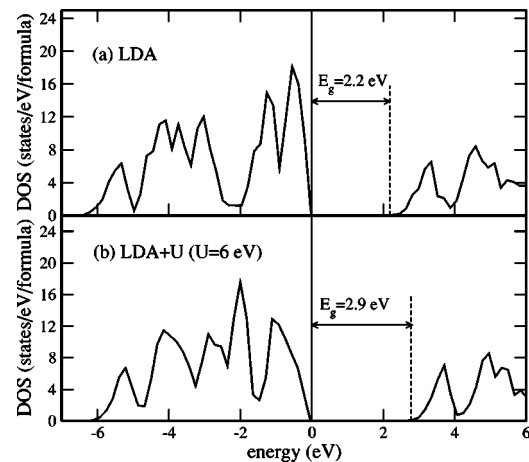


FIG. 3. Total density of states of the nondoped delafossite compound $YCuO_2$, within (a) the LDA and (b) the LDA+U approximations. The Fermi energy is represented by a vertical solid line.

ions= 0.95 eV),²⁵ and $U = E(d^{m+1}) + E(d^{m-1}) - 2E(d^m)$ is the Hubbard parameter, describing the additional energy cost to accommodate an extra electron on a particular site. However, U is a renormalized quantity and contains effects due to screening from other types of electrons, e.g., 4s and 4p from the transition metal atoms, as well as electrons from nearest-neighbor atoms, namely oxygen atoms. As a result, additional penalty energies are obtained on the LDA eigenvalues. They correspond to the expected corrections due to the strong one-site Coulomb repulsion of the d -electrons of the metal in the oxide.

A previous calculation of the electronic structure of this system was made by Mattheiss within the LAPW and TB method:²⁶ a metallic nonmagnetic ground state was found, as expected when Coulomb interactions are not explicitly included. Two important conclusions have been derived from this calculation: the dominant orbital character at the Fermi level is $|3z^2 - r^2\rangle$ and the appearance of an O1 impurity band. However, an insulating and magnetic ground state, which is the purpose of our calculation, can only be obtained if the Coulomb correlations are better taken into account.

It is still difficult to find a correct procedure to evaluate U and J for compounds.²⁵ To make a choice of U and J , we made a preliminary investigation of their influence on the calculated electronic properties of the nondoped $YCuO_2$ compound. Two density of states (DOS) are considered at the calculated equilibrium volume of $YCuO_2$ within the LDA in Fig. 3(a), and LDA+U in Fig. 3(b), namely 14.83 and 14.70 $\text{\AA}^3/\text{atom}$. Note that LDA+U does not strongly modify the shape of the DOS and a difference of $U-J=5$ eV was found to recover the experimental band-gap width of the nondoped compound, i.e., 3 eV, obtained by x-ray absorption.¹ This difference $U-J$ was kept fixed to study the doped compound since U is an on-site quantity, unexpected to change significantly as oxygen atoms are inserted in the Cu planes. Numerical integrations in the Brillouin zone (BZ) were performed by means of the Hermite-Gaussian method²⁷ with $N=1$ and a smearing parameter $\sigma=0.2$ eV. Four irreducible k -points (16 in the full BZ) were found necessary for differences of total energies and magnetic moments of our 72

TABLE I. Atomic volume (Ω), lattice parameter (a), and axial ratios (b/a and c/a) of $\text{YCuO}_{2.5}$ obtained within the LDA+U compared to x-ray synchrotron radiation and neutron scattering measurements. Relaxed position of inequivalent atoms of the primitive cell (space group : $Pnma$) are added.

		Lattice parameters		
		LDA+U	X-ray ^a	Neutron ^a
Ω ($\text{\AA}^3/\text{at.}$)		13.21	13.80	13.77
a (\AA)		6.131	6.196	6.189
b/a		1.795	1.810	1.811
c/a		1.150	1.154	1.155
Atom(site)	Position of atoms (direct coordinates)	LDA+U	X-ray ^a	Neutron ^a
Y(8d)	x	0.752	0.754	0.754
	y	0.023	0.022	0.023
	z	0.119	0.121	0.118
Cu1(4c)	x	0.064	0.070	0.079
	y	0.250	0.250	0.250
	z	0.157	0.147	0.148
Cu2(4c)	x	0.594	0.592	0.597
	y	0.250	0.250	0.250
	z	0.887	0.880	0.880
O1(4c)	x	0.751	0.743	0.746
	y	0.250	0.250	0.250
	z	0.116	0.108	0.115
O2(4c)	x	0.100	0.107	0.104
	y	0.089	0.086	0.088
	z	0.111	0.111	0.109
O3(4c)	x	0.567	0.578	0.567
	y	0.089	0.090	0.088
	z	0.854	0.847	0.857

^aFrom Ref. 3.

atoms cell to converge within 10^{-3} eV (6.25×10^{-5} eV per $\text{YCuO}_{2.5}$ formula) and $0.01\mu_B$, respectively.

To optimize the geometry of the cells, we have performed internal relaxation of the atomic positions for various volumes using the Hellmann-Feynman theorem. We have considered the atomic coordinates as fully relaxed as the noise in the individual forces is less than 0.005 eV/ \AA .

III. RESULTS

A. Lattice parameters, electronic structure, and magnetic moments from first-principles

First, we want to outline that the structural parameters and Cu positions in the compound are not very sensitive to the magnetic ordering, as verified by the calculations. Consequently, the analysis of the crystallographic data of $\text{YCuO}_{2.5}$ is performed in the ferromagnetic configuration. The energy E^α of all the other magnetic configurations (α) were thus calculated using these frozen lattice parameters and relaxed positions. Table I displays the calculated atomic volume, lattice parameters, and relaxed positions of atoms in $\text{YCuO}_{2.5}$.

They are compared to recent x-ray synchrotron radiation and neutron scattering measurements.³ The calculated equilibrium atomic volume of $\text{YCuO}_{2.5}$ is found slightly underestimated with $13.21 \text{ \AA}^3/\text{atom}$ compared to the experimental value of $13.8 \text{ \AA}^3/\text{atom}$. As the b/a and c/a axial ratios are well-predicted by calculations (see Table I), this discrepancy of the equilibrium volume with respect to the experiments may be attributed to the usual LDA underestimation of volume.

An excellent agreement is found (more specifically with neutron scattering measurements) for the positions of Y, Cu2, O1, O2, and O3 atoms. However, calculations are less good for Cu1 atoms for which the discrepancy between the experimental and calculated positions is 6% for x and z components. Nevertheless, such calculated values are still acceptable since a discrepancy of comparable magnitude is also observed for Cu1 atoms between x-ray and neutron measurements (Table I). To conclude, note that the overall change between the energy of the fully relaxed cell and the nonrelaxed cell built upon the experimental data (for a given magnetic configuration) is found to be less than 0.0006 eV/

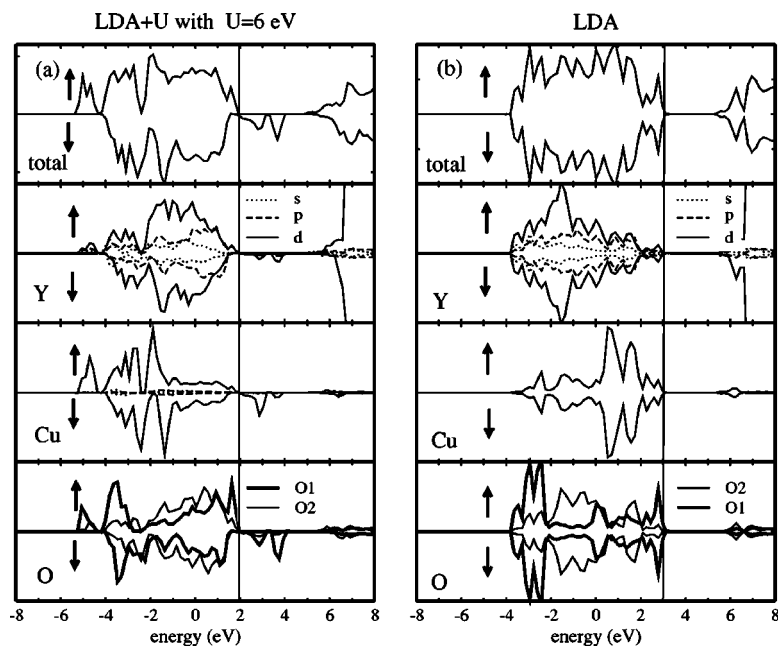


FIG. 4. Total and site-projected density of states of $\text{YCuO}_{2.5}$. O2 (O3) atoms are the oxygen atoms defining the octahedron enclosing Y atoms, while O1 atoms are the oxygen atoms resulting from the doping of delafossite YCuO_2 . They are located in the Cu planes. The Fermi energy is represented by a vertical line. The density of states of O3 atoms is very close to the one of O2, and it is not represented. Minority and majority spin channels are spotted with \uparrow and \downarrow symbols, respectively.

formula. Hence we chose to use the relaxed set to determine the exchange-coupling interactions.

First-principles results show that $\text{YCuO}_{2.5}$ is a magnetic half-metal within the LDA+U approximation [Fig. 4(a)], however, with a very low density at the Fermi level. This result is not inconsistent with transport data on polycrystalline $\text{YCuO}_{2.51}$ which suggest that $\text{YCuO}_{2+\delta}$ becomes a semiconductor for $\delta=1/2$ with a small band-gap width of ~ 0.23 eV compared to the 3eV of YCuO_2 .^{1,3}

Note from Fig. 4(b) that the compound is found to be a nonmagnetic insulator ($E_g \sim 2$ eV) within the LDA. Thus LDA fails to induce magnetism in $\text{YCuO}_{2.5}$ and to lower the band-gap width from 3.0 to 0.23 eV when YCuO_2 is doped. This inability of the LDA to describe the features of Mott insulators (magnetism and gap) finds its origin in the well-known prejudice caused by the homogeneous electron gas description only piloted by Hund's rule interactions, while in reality the on-site Coulomb interactions (provided by LDA+U) are mainly responsible for these properties.^{28,29}

Within the LDA+U, most of the interstitial O1(*p*) levels fall within the range of O2(*p*) and O3(*p*) states [Fig. 4(a)]. However, our calculations predict that the self-doping O1 atoms produce additional impurity-type states in the host insulator gap. This was already emphasized by the nonmagnetic tight-binding calculations of Mattheiss.²⁶ The shape of the DOS projected on O1 and Cu sites allows one to assess unambiguously that the formation of these *p*-impurity levels is due to their hybridization with *d* states of Cu atoms. On the contrary, the lack of similarities between the shape of the projected DOS on O2 or O3 atoms and the DOS of Cu atoms suggests that the octahedra of oxygens surrounding Y atoms may interact very weakly with Cu planes. Let us mention that a noticeable hybridization is obtained between the Y(*d*) states and *p*-states of their surrounding O2 and O3 atoms.

The calculation of the projected magnetic moments enclosed in the augmentation spheres centered on each Cu and O1 atoms shows that (i) the difference of magnitude between

the magnetic moments of Cu1 and Cu2 atoms is less than $0.05\mu_B$ for a given magnetic configuration and that (ii) the difference between the magnetic moments of either Cu1 or Cu2 atoms considered in the ferromagnetic and AF configurations was less than $0.1\mu_B$. From these values, we can consider that the Heisenberg model is appropriate for this system since the doped $\text{YCuO}_{2.5}$ compound is expected to have well-localized moments on the Cu atoms and the moments are unlikely to change dramatically between Cu atoms. Moreover, note from Table II that the calculated total moments of the 16 Cu atoms cell is always found to be an even multiple of $1\mu_B$. If we consider O1-Cu1-O1 and O1-Cu2 groups as extended sites, the magnetization of the system is exactly recovered by summing up (with the appropriate sign) a spin-1/2 per extended site.

B. Exchange-coupling parameters

We calculated the total energies of 15 different collinear magnetic configurations using cells containing 36 (primitive cell) or 72 (double cell) atoms. These 15 configurations are described in Table III. For each of these configurations the magnetic energy [Eq. (2)] can be written as a combination of the eight exchange interactions, as shown in Table III.

In the following, all the energies of the magnetic configurations α are defined with respect to the ferromagnetic energy ($\alpha=1$), yielding the excess energy $\Delta E^{\alpha/1} = E^\alpha - E^1$, where E^α is defined in Eq. (2). The exchange-coupling parameters were fitted to the 15 first-principles excess energies by minimizing the squared error between these latter and those predicted by Eq. (2).

The expression of the excess energies for the 15 investigated magnetic configurations as a function of the exchange-coupling parameters (J_i), as well as their first-principles and Heisenberg model predicted values, are shown together in Table II for three different fits: The first one involves all the pair spin clusters (fit 1), fit 2 skips interplane interactions and

TABLE II. *Ab initio* excess energies, $\Delta E^{\alpha/1}$ (in meV/formula), compared to excess energies predicted from the three fit Heisenberg models for the 15 investigated magnetic configurations. Fit 1 uses all the interactions, fit 2 skips interactions between planes (J_6 , J_7 , and J_8), and fit 3 just retains the inner-chain interactions. The corresponding first-principles total spin moment of the 16 Cu atoms cell are added for each configuration α .

Energy (meV/formula)	Total moment (μ_B)	<i>Ab initio</i>	Heisenberg		
			fit 1	fit 2	fit 3
$\Delta E^{1/1}$	16.0	0	0	0	0
$\Delta E^{2/1}$	0.0	+8.2	+7.2	0.0	0.0
$\Delta E^{3/1}$	0.0	-17.7	-17.4	-18.2	-16.2
$\Delta E^{4/1}$	0.0	-18.4	-19.2	-18.2	-16.2
$\Delta E^{5/1}$	0.0	-40.0	-40.3	-38.5	-39.2
$\Delta E^{6/1}$	0.0	-38.2	-37.1	-38.5	-39.2
$\Delta E^{7/1}$	0.0	+9.3	+10.2	+10.0	0.0
$\Delta E^{8/1}$	14.0	-8.9	-8.7	-9.8	-11.2
$\Delta E^{9/1}$	12.0	-17.6	-17.4	-19.6	-22.4
$\Delta E^{10/1}$	10.0	-22.7	-24.7	-25.1	-27.3
$\Delta E^{11/1}$	7.9	-22.0	-22.8	-20.9	-26.4
$\Delta E^{12/1}$	6.0	-25.1	-26.8	-26.2	-24.5
$\Delta E^{13/1}$	4.0	-29.8	-29.3	-30.3	-29.4
$\Delta E^{14/1}$	2.0	-34.6	-34.46	-34.4	-34.3
$\Delta E^{15/1}$	0.0	-77.0	-76.34	-76.0	-73.3

finally, fit 3 only retains the pair spin clusters inside chains. The corresponding exchange-coupling parameters are given in Table IV. The agreement is very good for the complete set of parameters (fit 1) with an rms error between the first-principles and Heisenberg model which does not exceed 1

meV per formula unit. The intrachain interactions (J_1 , J_2 , and J_3) are found to be larger than the interactions between chains and two orders of magnitude larger than the interactions between planes. Fits 2 and 3 show that these three interactions are sufficient to predict the energy of the most

TABLE III. Expression of the excess energies $\Delta E^{\alpha/1}$ (divided by μ^2) as a function of the Heisenberg model parameters for the 15 investigated magnetic configurations α . These latter are defined by the series of signs + (for $S=+\mu$) and - (for $S=-\mu$) corresponding to the sign of the moments of the 16 Cu atoms as labeled in Fig. 1, following the same order.

Energy	Magnetic configuration	Heisenberg model
$\Delta E^{1/1}$	+++++	0
$\Delta E^{2/1}$	-----+	$-J_6-4J_7-J_8$
$\Delta E^{3/1}$	+-+--	$-(J_1+J_2+J_3)-J_5-J_6-2J_7-J_8$
$\Delta E^{4/1}$	+-+--	$-(J_1+J_2+J_3)-J_5-2J_7$
$\Delta E^{5/1}$	-+--+	$-2J_2-(J_3+J_4)-J_6-J_8$
$\Delta E^{6/1}$	-+--+	$-2J_2-(J_3+J_4)-4J_7$
$\Delta E^{7/1}$	+--+-	$-J_4-J_5-\frac{1}{2}J_6-2J_7-\frac{1}{2}J_8$
$\Delta E^{8/1}$	-++++	$-\frac{1}{4}(J_1+J_2)-0.125(J_3+J_4)-\frac{1}{4}J_6-\frac{1}{2}J_7$
$\Delta E^{9/1}$	-++++	$-\frac{1}{2}(J_1+J_2)-\frac{1}{4}(J_3+J_4)-\frac{1}{2}J_6-J_7$
$\Delta E^{10/1}$	-++++	$-\frac{1}{2}J_1-\frac{3}{4}J_2-\frac{3}{8}(J_3+J_4)-\frac{1}{4}J_5-\frac{1}{2}J_6-J_7-\frac{1}{4}J_8$
$\Delta E^{11/1}$	-++++	$-\frac{3}{4}(J_1+J_2)-\frac{1}{2}(J_3+J_4)-\frac{1}{4}J_5-\frac{1}{4}J_6-\frac{3}{2}J_7-\frac{1}{4}J_8$
$\Delta E^{12/1}$	+++--	$-1.25J_2-0.625(J_3+J_4)-\frac{3}{4}J_5-\frac{5}{2}J_7-\frac{1}{4}J_8$
$\Delta E^{13/1}$	+++--	$-\frac{3}{2}J_2-\frac{3}{4}(J_3+J_4)-\frac{1}{2}J_5-3J_7$
$\Delta E^{14/1}$	+++--	$-1.75J_2-0.875(J_3+J_4)-\frac{1}{4}J_5-\frac{7}{2}J_7-\frac{1}{4}J_8$
$\Delta E^{15/1}$	-+--+	$-J_1-J_2-\frac{1}{2}J_6-2J_7-\frac{1}{2}J_8$

TABLE IV. Exchange-coupling parameters (in meV/formula) for the three different fits to the *ab-initio* data.

	J_1	J_2	J_3	J_4	J_5	J_6	J_7	J_8
fit 1	23.34	56.62	-61.27	-9.70	3.10	-7.06	-1.30	5.07
fit 2	19.97	56.05	-60.68	-12.94	2.90			
fit 3	25.10	48.16	-57.08					

stable spin arrangements. However, we show below in Sec. III C that interchain interactions J_4 also play an important role.

It is interesting to relate these magnetic interactions to the exchange paths in the lattice. In spite of the suggested important z -orbital occupation,²⁶ the interplane interactions appear to be negligible. The NN AF interactions yield an interaction ratio $J_1/J_2 < 0.5$, indicating the absence of spin gap in the sawtooth lattice. As suggested⁶ from the measured angles and distances³ the J_1 interactions between Cu1-O-Cu1 bonds (bases of the triangles) are weaker than those for the Cu1-O-Cu2 base-vertex bond J_2 . The most striking result here is the relevance of the ferromagnetic interaction J_3 , difficult to predict without performing the present calculations. This huge interaction is not expected since there is no trivial oxygen mediated exchange path. It is certainly due to a direct exchange between Cu1 and Cu2 type ions, and it completely modifies the initial picture proposed for this system.

C. Magnetic ground-state at low temperature

As a first step, we focus on the one-dimensional model including the ferromagnetic J_3 interaction in order to show its influence on the determination of the ground state. To this purpose, we subjected our Ising spin-Hamiltonian to a “direct enumeration ground state search”³⁰ in which every spin configuration that can be constructed from a unit cell with N Cu sites is examined. We used cells with $N \leq 8$. We have validated the results of the direct enumeration search by performing standard Monte Carlo (MC) simulated annealing at low temperature. Simulations were performed with a one-dimensional supercell containing a total of 1000 spins. The number of Monte Carlo steps per spin was 300 000 for each temperature, and the first 150 000 were excluded from cal-

culations of the excess energy to allow for equilibration. MC calculations found the same ground state obtained with the direct enumeration search. This latter (configuration 16), which actually corresponds to the lowest collinear mean field energy state when only the three intrachain interactions are considered, is shown in Fig. 5.

The excess energy of the new state (Fig. 5) was found to be equal to -84.5 meV/formula, taking into account only the intrachain interactions. In this new state, all J_3 interactions are satisfied, and $3/4$ of the J_2 interactions, while in state 15 shown in Fig. 6, all J_3 and half of the J_2 interactions are satisfied. In fact since J_3 and J_2 are the largest interactions, these two states correspond to the best compromise: this is the reason why these two configurations are much lower in energy than all others. However, let us mention that the energy difference between these two states, namely -11.2 meV/formula using fit 3, is of the order of the total contribution of the interchain interactions (10 meV/formula). Therefore the two magnetic configurations (Figs. 5 and 6) may be considered as degenerate. A final *ab initio* calculation has confirmed this quasidegeneracy (10 meV/formula).

With these values of the exchange interactions, it would be possible to study the magnetic properties of this system including also noncollinear configurations. It would be also interesting to extend the MC simulations to the two-dimensional Hamiltonian, since the J_4 interaction is of the same order of the energy difference between configurations 15 and 16. Such calculations are beyond the scope of this paper. Of course long range ordering will not be observed since the system is not three-dimensional, but the magnetic short range correlations of $YCuO_{2.5}$ will be governed by the underlying magnetic structures of Figs. 5 and 6. Experimentally, no magnetic ordering has been found in this system neither by μ sR³¹ nor by neutrons³² even at low temperature, we suggest that this is due to its low-dimensional character.

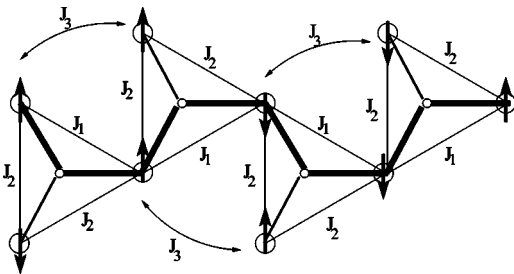


FIG. 5. Configuration 16 corresponding to the magnetic ground state obtained from our fitted Ising model (fit 3) retaining the inner-chain interactions only (J_1 , J_2 , and J_3). This configuration adopts a spin geometry in agreement with the sign of every J_3 and $3/4$ of the J_2 interactions and cancels contributions of J_1 .

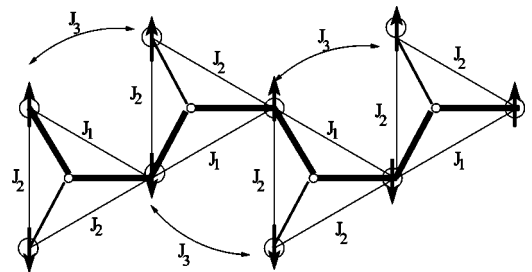


FIG. 6. Second lowest state (configuration 15 from Tables II and III) obtained from our fitted Heisenberg model (fit 3). This configuration adopts a spin geometry in agreement with the sign of every J_3 and J_2 interactions and cancels contributions of J_1 .

On the other hand, the susceptibility maximum observed at 400 K³² is consistent with the magnitude that we obtain for the exchange interactions.

IV. CONCLUSIONS

We have taken advantage of the precise determination of the crystallographic structure of YCuO_{2.5} to calculate the exchange interactions values using first-principles methods. We would like to point out that the *ab initio* methods are well suited to investigate the properties of this system because (i) the magnetic moments on Cu are almost independent of the magnetic configuration, and (ii) we have been able to fit the magnetic energy of the 16 different magnetic configurations with eight parameters with good accuracy. This confirms that Eq. (2) can be used to go further in the study of the magnetic properties of YCuO_{2.5}. Our results explain the absence of magnetic ordering: the interplane interactions are negligible while the interchain interactions are much smaller than the intrachain interactions, leading to a low-dimensional behavior. Within the chains of triangles, the ratio of the base-base

(J_1) and base-vertex (J_2) interactions is ≤ 0.5 where no gap is expected in the sawtooth lattice. Furthermore, an unexpected third neighbor ferromagnetic interaction appears to be of the same order and it will change the magnetic correlations. Since no oxygen is involved in this case, we can say that it most probably corresponds to direct Cu-Cu exchange interactions.

We can conclude that the delafossite YCuO_{2.5} presents an important ferromagnetic intrachain interaction in addition to the AF superexchange ones. So, it will show short range correlations related to the magnetic structures 15 and 16, shown in Figs. 5 and 6. The role played by the interchain J_4 interaction must be further investigated. These features should be confirmed by further experiments and calculations involving two-dimensional Hamiltonians but also noncollinear magnetism.

ACKNOWLEDGMENT

The computations presented in this paper were performed on the cluster PHYNUM (CIMENT, Grenoble).

*Electronic address: olivier.lebacq@grenoble.cnrs.fr

- ¹R. J. Cava, H. W. Zandbergen, A. P. Ramirez, H. Takagi, C. T. Chen, J. J. Krajewski, W. F. Peck, Jr., J. V. Waszczak, G. Meigs, R. S. Roth, and L. F. Schneemeyer, *J. Solid State Chem.* **104**, 437 (1993).
- ²M. E. Simón, A. A. Aligia, and M. D. Núñez-Regueiro, *Phys. Rev. B* **51**, 15 642 (1995); M. D. Núñez-Regueiro, C. Lacroix, and B. Canals, *ibid.* **54**, R736 (1996).
- ³G. Van Tendeloo, O. Gårlea, C. Darie, C. Bougerol-Chaillout, and P. Bordet, *J. Solid State Chem.* **156**, 428 (2001); O. Gårlea, Ph. D. thesis, University of Grenoble, 2001.
- ⁴T. Nakamura and K. Kubo, *Phys. Rev. B* **53**, 6393 (1996), and references therein.
- ⁵D. Sen, B. S. Shastry, R. E. Walsted, and R. J. Cava, *Phys. Rev. B* **53**, 6401 (1996).
- ⁶S. A. Blundell and M. D. Núñez-Regueiro, *J. Phys.: Condens. Matter* **16**, S791 (2004); *Eur. Phys. J. B* **31**, R453 (2003).
- ⁷B. S. Shastry and B. Sutherland, *Phys. Rev. Lett.* **47**, 964 (1981).
- ⁸D. Morgan, B. Wang, G. Ceder, and A. Van de Walle, *Phys. Rev. B* **67**, 134404 (2003).
- ⁹R. Dovesi, J. M. Ricart, V. R. Saunders, and R. Orlando, *J. Phys.: Condens. Matter* **7**, 7997 (1995).
- ¹⁰S. S. Peng and H. J. F. Jansen, *Phys. Rev. B* **43**, 3518 (1991).
- ¹¹S. H. Wei and A. Zunger, *Phys. Rev. B* **48**, 6111 (1993).
- ¹²N. M. Rosengaard and B. Johansson, *Phys. Rev. B* **55**, 14 975 (1997).
- ¹³Y. M. Zhou, D. S. Wang, and Y. Kawazoe, *Phys. Rev. B* **59**, 8387 (1999).
- ¹⁴J. T. Wang, L. Zhou, D. S. Wang, and Y. Kawazoe, *Phys. Rev. B* **62**, 3354 (2000).
- ¹⁵P. E. Blöchl, *Phys. Rev. B* **50**, 17 953 (1994).

- ¹⁶G. Kresse and D. Joubert, *Phys. Rev. B* **59**, 1758 (1999).
- ¹⁷G. Kresse and J. Hafner, *Phys. Rev. B* **47**, R558 (1993); G. Kresse, thesis, Technische Universität Wien, 1993; G. Kresse and J. Furthmüller, *Phys. Rev. B* **54**, 11 169 (1996).
- ¹⁸P. Hohenberg and W. Kohn, *Phys. Rev.* **136**, B864 (1964).
- ¹⁹W. Kohn and L. J. Sham, *Phys. Rev.* **140**, A1133 (1965).
- ²⁰S. H. Vosko, L. Wilk, and M. Nusair, *Can. J. Phys.* **58**, 1200 (1980).
- ²¹A. Rohrbach, J. Hafner, and G. Kresse, *J. Phys.: Condens. Matter* **15**, 979 (2003).
- ²²O. Bengone, M. Alouani, P. Blöchl, and J. Hugel, *Phys. Rev. B* **62**, 16 392 (2000).
- ²³V. I. Anisimov, J. Zaanen, and O. K. Andersen, *Phys. Rev. B* **44**, 943 (1991).
- ²⁴S. L. Dudarev, G. A. Botton, S. Y. Savrasov, C. J. Humphreys, and A. P. Sutton, *Phys. Rev. B* **57**, 1505 (1998).
- ²⁵I. V. Solovyev, P. H. Dedrichs, and V. I. Anisimov, *Phys. Rev. B* **50**, 16 861 (1994).
- ²⁶L. F. Mattheiss, *Phys. Rev. B* **48**, 18 300 (1993).
- ²⁷M. Methfessel and A. T. Paxton, *Phys. Rev. B* **40**, 3616 (1989).
- ²⁸V. I. Anisimov, M. A. Korotin, J. Zaanen, and O. K. Andersen, *Phys. Rev. Lett.* **68**, 345 (1992).
- ²⁹M. T. Czyżyk and G. A. Sawatzky, *Phys. Rev. B* **49**, 14 211 (1994).
- ³⁰L. G. Ferreira, S. H. Wei, and A. Zunger, *Int. J. Supercomput. Appl.* **5**, 34 (1991).
- ³¹P. Mendels, D. Bono, F. Bert, O. Garlea, C. Darie, P. Bordet, V. Brouet, M.-H. Jullien, A.-D. Hillier, and A. Amato, *J. Phys.: Condens. Matter* **16**, S799 (2004).
- ³²V. Simonet, R. Ballou, A. P. Murani, O. Garlea, C. Darie, and P. Bordet, *J. Phys.: Condens. Matter* **16**, S805 (2004).